Published OnlineFirst June 16, 2009; DOI: 10.1158/0008-5472.CAN-09-0112

Research Article

Ferritin Heavy Chain–Mediated Iron Homeostasis and Subsequent Increased Reactive Oxygen Species Production Are Essential for Epithelial-Mesenchymal Transition

Ke-Hua Zhang,[1] Hong-Yu Tian,[1] Xia Gao,[1] Wei-Wei Lei,[1] Ying Hu,[1] Dong-Mei Wang,[1] Xin-Chao Pan,[1] Mei-Lan Yu,[2] Gen-Jun Xu,[1,2] Fu-Kun Zhao,[1,2] and Jian-Guo Song[1]

[1]Laboratory of Molecular Cell Biology, Institute of Biochemistry and Cell Biology, Shanghai Institutes for Biological Sciences, Chinese Academy of Sciences, Shanghai, China and [2]College of Life Science, Zhejiang Sci-Tech University, Hangzhou, China

Abstract

The epithelial-mesenchymal transition (EMT) plays a critical role in tumor progression. To obtain a broad view of the molecules involved in EMT, we carried out a comparative proteomic analysis of transforming growth factor-β1 (TGF-β1)–induced EMT in AML-12 murine hepatocytes. A total of 36 proteins with significant alterations in abundance were identified. Among these proteins, ferritin heavy chain (FHC), a cellular iron storage protein, was characterized as a novel modulator in TGF-β1–induced EMT. In response to TGF-β1, there was a dramatic decrease in the FHC levels, which caused iron release from FHC and, therefore, increased the intracellular labile iron pool (LIP). Abolishing the increase in LIP blocked TGF-β1–induced EMT. In addition, increased LIP levels promoted the production of reactive oxygen species (ROS), which in turn activated p38 mitogen-activated protein kinase. The elimination of ROS inhibited EMT, whereas H_2O_2 treatment rescued TGF-β1–induced EMT in cells in which the LIP increase was abrogated. Overexpression of exogenous FHC attenuated the increases in LIP and ROS production, leading to a suppression of EMT. We also showed that TGF-β1–mediated down-regulation of FHC occurs via 3′ untranslated region–dependent repression of the translation of FHC mRNA. Moreover, we found that FHC down-regulation is an event that occurs between the early and highly invasive advanced stages in esophageal adenocarcinoma and that depletion of LIP or ROS suppresses the migration of tumor cells. Our data show that cellular iron homeostasis regulated by FHC plays a critical role in TGF-β1–induced EMT. [Cancer Res 2009;69(13):5340–8]

Introduction

Epithelial-mesenchymal transition (EMT) is a process by which epithelial cells lose epithelial polarity and cell-cell contact and acquire a mesenchymal morphology to become more motile and invasive. It is implicated in embryonic development, wound repair, and fibrotic diseases, and it contributes to tumor-invasive phenotypes and metastasis (1). EMT is characterized by the dramatic morphologic transition, disruption, or attenuation of tight junctions and adhesion junctions, with diminished E-cadherin and zonula occludens-1 (ZO-1) expression and up-regulation of mesenchymal markers, such as fibronectin and vimentin. Transforming growth factor-β (TGF-β) is a potent EMT inducer. Increased TGF-β expression has been observed in many tumors, and it is regarded as an important indicator of cancer progression because it contributes to tumor invasion and metastasis through the induction of EMT (2, 3). It has become increasingly evident that both TGF-β and EMT are involved in the same various physiologic and pathologic events. Smad family proteins that cooperate with other signaling molecules, such as Ras–mitogen-activated protein kinase (MAPK), phosphatidylinositol 3-kinase, nuclear factor-κB, and Wnt (4), and transcriptional factors, such as Snail (5), Slug (6), Twist (7), and Zeb1/2 (8), have emerged as important factors in TGF-β–induced EMT in some types of epithelial cells.

In vertebrates, ferritin, the main cellular iron storage protein, is composed of 24 peptides of two subunits: ferritin heavy chains (FHC) and ferritin light chains (FLC). These subunits assemble into a large, spherical complex with a cavity in which iron molecules are stored (9). FHC has a ferroxidase function. Excess cellular iron is catalyzed by FHC into the nontoxic ferric form and stored in a ferritin complex, maintaining normal iron homeostasis. In addition, FHC is the major controller of the labile iron pool (LIP; ref. 10). Repression of FHC leads to iron release from the ferritin complex and an increase in the cellular LIP (11, 12), whereas overexpression of FHC can decrease LIP (13, 14). LIP is a pool of chelatable and redox active iron (10). A high level of LIP results in oxidative damage by catalyzing reactive oxygen species (ROS) generation in mitochondria. Regulation of LIP levels by FHC may be involved in important biological events, such as apoptosis, cell cycle arrest, and inflammation (15, 16). However, it remains unknown whether TGF-β1 can regulate FHC and LIP and whether FHC and LIP are implicated in TGF-β1–induced EMT.

To investigate the alteration of global protein profiles and search for the specific proteins involved in TGF-β1–induced EMT, two-dimensional electrophoresis coupled with a tandem mass spectrometry method was applied in this study. Among the significantly altered expressed proteins, FHC was found to be involved in TGF-β1–induced EMT. Further investigation showed that TGF-β1 repressed the *de novo* synthesis of FHC at the translational level and led to a dramatic decrease in the level of FHC, which plays an important role in TGF-β1–induced EMT by increasing the LIP level and ROS generation.

Materials and Methods

Cell culture and transfection. AML-12 cells were grown in a 1:1 mixture of DMEM and Ham's F12 medium containing 10% FCS and supplemented with insulin-transferrin-selenium X, dexamethasone (40 ng/mL), penicillin

Note: Supplementary data for this article are available at Cancer Research Online (http://cancerres.aacrjournals.org/).

K-H. Zhang and H-Y. Tian contributed equally to this article.

Requests for reprints: Jian-Guo Song or Fu-Kun Zhao, Institute of Biochemistry and Cell Biology, Shanghai Institutes for Biological Science, Chinese Academy of Sciences, 320 Yue-Yang Road, Shanghai 200031, China. Phone/Fax: 86-21-54921167; E-mail: jgsong@sibs.ac.cn or fkzhao@sibs.ac.cn.

doi:10.1158/0008-5472.CAN-09-0112

Published OnlineFirst June 16, 2009; DOI: 10.1158/0008-5472.CAN-09-0112

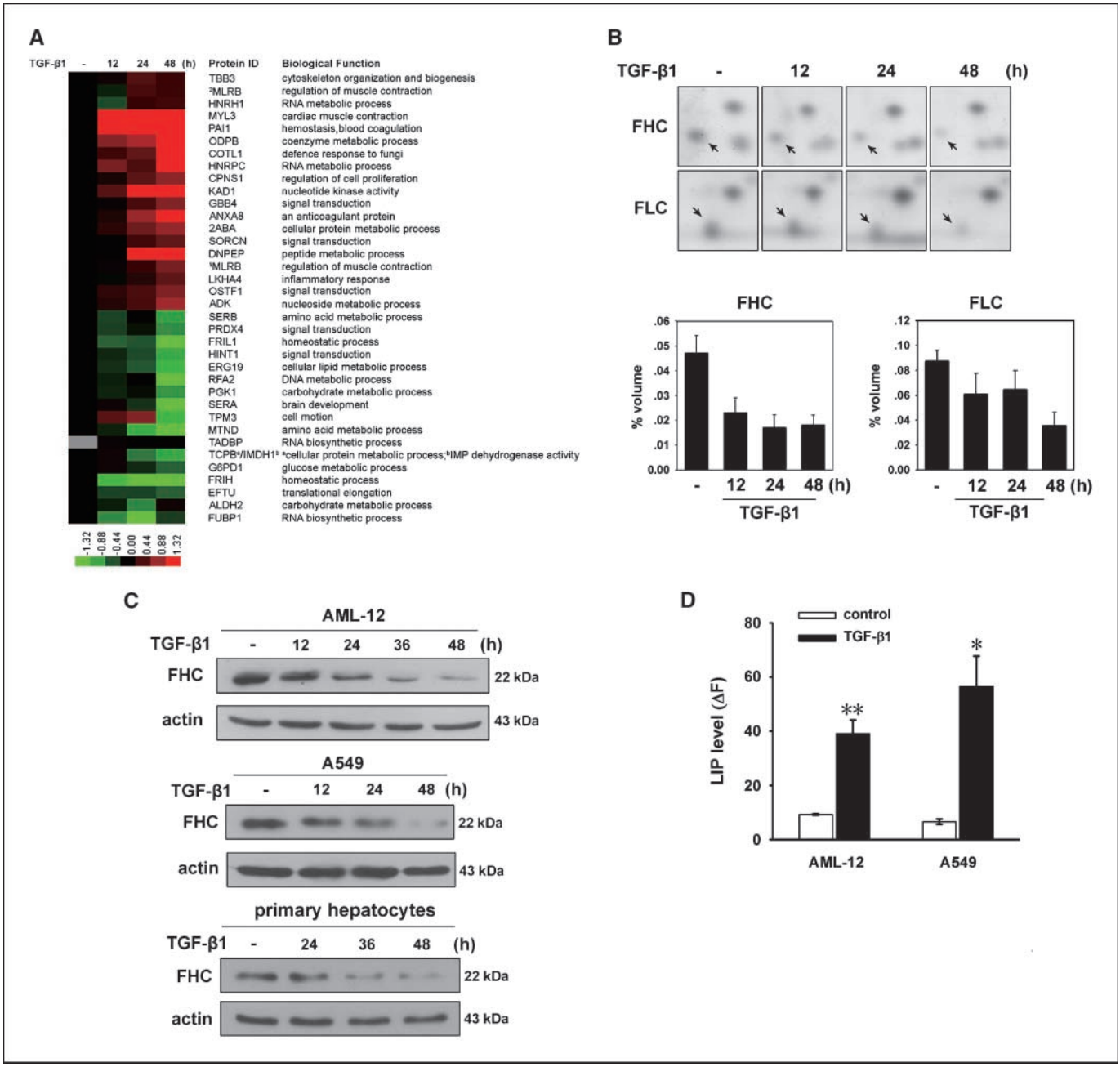

Figure 1. TGF-β1–induced FHC down-regulation and LIP increase. *A,* the different expression levels of proteins in TGF-β1–induced EMT in AML-12 cells, identified by proteomic analysis, are shown in cluster maps. *Black,* control; *red,* up-regulated proteins; *green,* down-regulated proteins; *gray,* expression level is 0. *B, top,* zoom-in images of FHC and FLC from two-dimensional PAGE; *bottom,* statistical analysis of FHC and FLC expression levels and results from three independent experiments were calculated. *C,* AML-12, A549, and primary hepatocytes were treated with TGF-β1 (5, 3, and 5 ng/mL, respectively). The FHC expression level was examined by immunoblotting. *D,* AML-12 and A549 were treated with TGF-β1 (5 and 3 ng/mL, respectively) for 24 h. LIP levels were determined. **, $P \leq 0.001$; *, $P \leq 0.05$.

(100 units/mL), and streptomycin (100 mg/mL). A549 cells were grown in DMEM containing 10% FCS supplemented with penicillin (100 units/mL) and streptomycin (100 mg/mL). The cells were incubated at 37°C in a humidified atmosphere of 5% CO_2 until 30% to 50% of confluence were reached. Transfection was carried out using Lipofectamine as transfection reagent according to the manufacturer's instructions.

Reverse transcription-PCR and RNA interference. Total RNA was extracted from AML-12 cells using Trizol reagent. Then mRNA was reverse transcribed at 42°C for 30 min using ReverTra Ace-α (Toyobo). The primers for amplification of FHC, glyceraldehyde-3-phosphate dehydrogenase (GAPDH), and FHC-complete cDNA are listed in Supplementary Table S1. FHC-complete cDNA was cloned into pcDNA 3.1(−)/myc-His A at the BamHI and HindIII sites. pPGKsuper was used for the expression of small interfering RNA (siRNA). The target sequence of FHC is 5′-AATACTTTCTC-CACCAATCTC-3′; the sequence of mock is 5′-AACCTCTATCTCTCATA-CATC-3′ and was inserted into the pPGKsuper vector at the BglII and HindIII sites.

Examination of LIP. LIP was examined according to the methods described by Prus and Fibach (17). Briefly, cells were trypsinized, washed twice with 0.5 mL of PBS, and incubated at a density of 0.5×10^6 to 1×10^6/mL for 15 min at 37°C with 0.15 μmol/L calcein-acetoxymethyl ester (AnaSpec). Then, the cells were washed twice with 0.5 mL of PBS and either incubated

Published OnlineFirst June 16, 2009; DOI: 10.1158/0008-5472.CAN-09-0112

with deferiprone (L1, 100 μmol/L) for 1 h at 37°C or left untreated. The cells were analyzed with a flow cytometer (Becton Dickinson FACSCalibur). Calcein was excited at 488 nm, and fluorescence was measured at 525 nm. The difference in the cellular mean fluorescence with and without deferiprone incubation reflects the amount of LIP.

Measurements of cellular ROS. Cells were trypsinized, suspended in 0.5 mL of serum-free DMEM/F12 medium, incubated with 10 μmol/L 2′,7′-dichlorfluorescein (DCFH)–diacetate at 37°C for 20 min and washed thrice with serum-free DMEM/F12 medium. The fluorescence of the cells was measured with a flow cytometer (Becton Dickinson FACSCalibur). DCFH was excited at 488 nm, and fluorescence was measured at 525 nm. The mean fluorescence per cell was used for comparison.

Immunofluorescent staining and confocal microscopy. Cells were grown on glass slides and treated as indicated. The slides were quickly

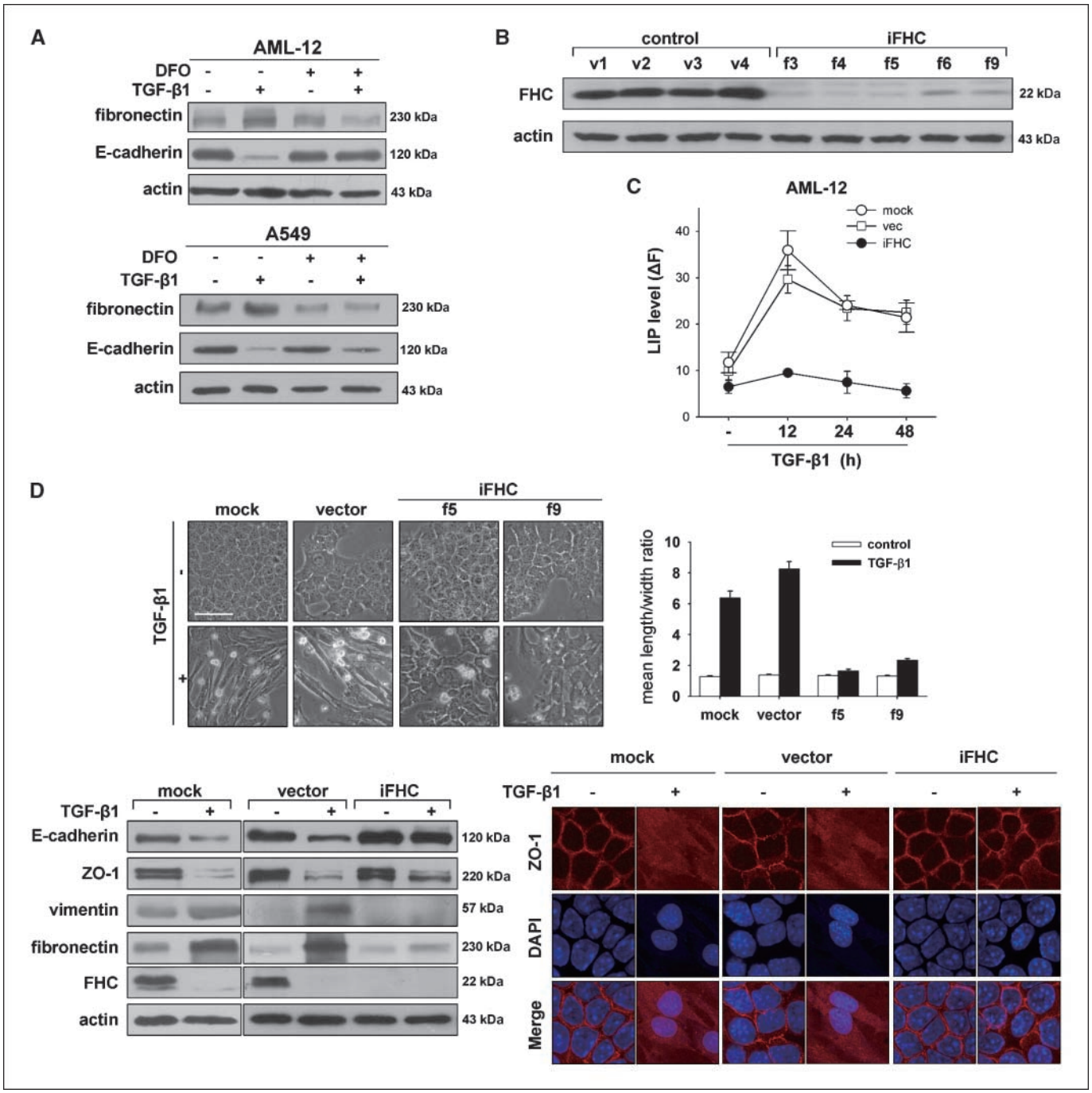

Figure 2. The role of LIP increase in TGF-β1–induced EMT. *A,* AML-12 and A549 cells were treated with TGF-β1 (5 and 3 ng/mL, respectively) with or without DFO (100 μmol/L) for 48 h. EMT was examined by immunoblotting of fibronectin and E-cadherin. *B,* FHC levels in different AML-12 stable clones transfected with empty pPGKsuper vectors (*control*) or FHC RNAi plasmids (*iFHC*). *C,* cellular LIP levels of mock, control (*v1, v2, v4*), and iFHCs (*f3, f4, f9*) after TGF-β1 (5 ng/mL) treatment in AML-12 cells. Results from three independent experiments were calculated. *D, top,* morphologic changes and the average length/width ratio in mock cells, empty vector–transfected cells, and FHC RNAi plasmids–transfected cells after TGF-β1 treatment (5 ng/mL, 48 h). *Bar,* 50 μm. *Bottom left,* E-cadherin, ZO-1, vimentin, fibronectin, and FHC were determined by immunoblotting in control and iFHC cells treated with TGF-β1. *Bottom right*, immunostaining of ZO-1 in transfected cells treated with TGF-β1 (5 ng/mL, 36 h). Nuclei were stained with DAPI. Representative results from three independent experiments. *Bar,* 20 μm.

Published OnlineFirst June 16, 2009; DOI: 10.1158/0008-5472.CAN-09-0112

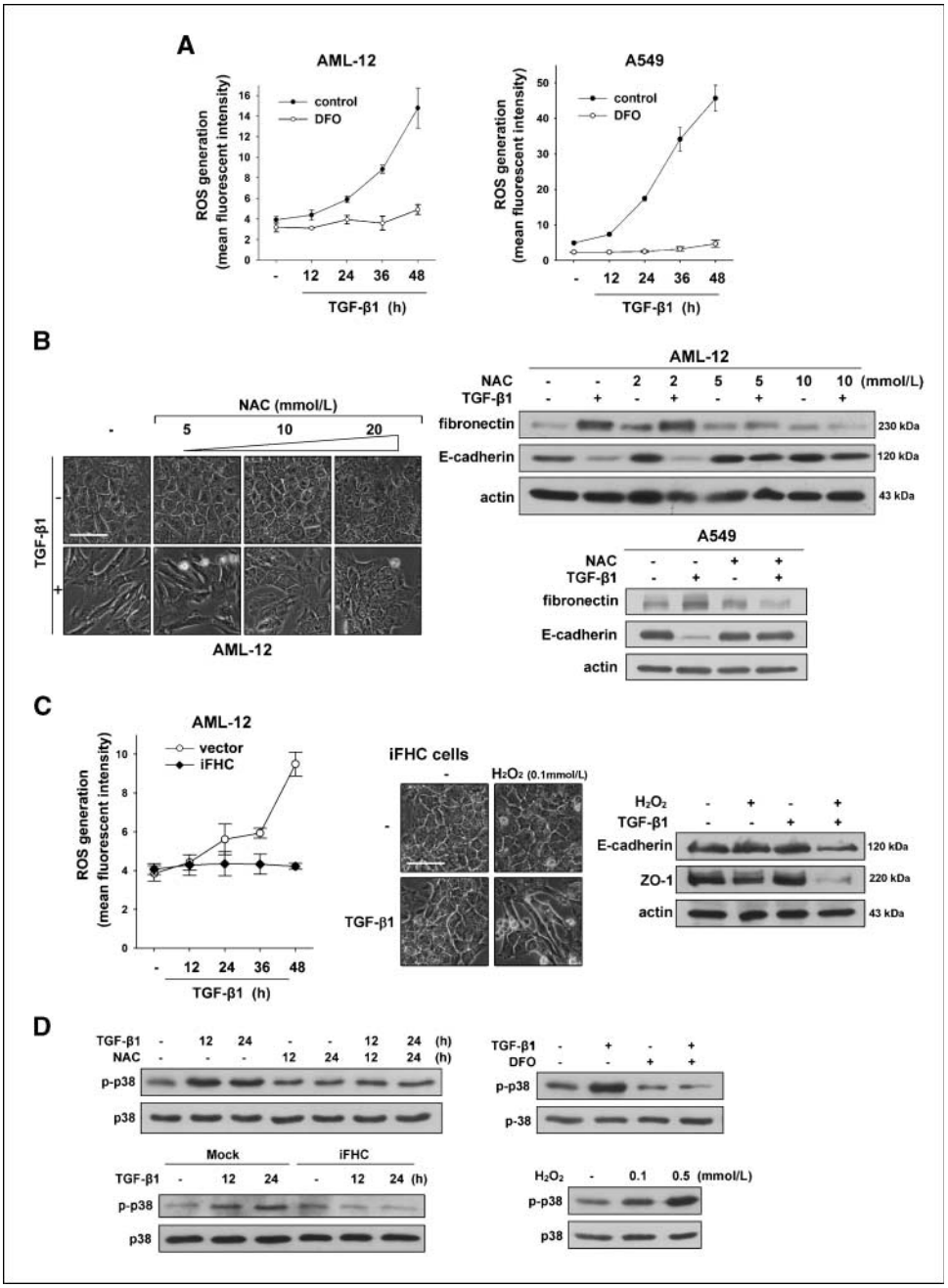

Figure 3. The role of increased LIP-induced ROS production in TGF-β1–induced EMT. *A,* ROS levels in response to TGF-β1 treatment in AML-12 (5 ng/mL) and A549 (3 ng/mL) in the presence or absence of DFO (100 μmol/L). *B,* morphologic changes of AML-12 cells after TGF-β1 treatment (5 ng/mL, 48 h) with or without NAC (*left*). Fibronectin and E-cadherin were determined by immunoblotting in AML-12 and A549 treated with TGF-β1 (5 and 3 ng/mL, respectively) with or without NAC (10 mmol/L in A549; *right*). *C, left,* ROS levels in control (*v1–v4*) and iFHC (*f3, f4, f5, f6, f9*) cells treated with TGF-β1 (5 ng/mL). Results of five independent experiments were calculated. *Middle* and *right,* iFHC cells (*f9*) were treated with TGF-β1 for 48 h in the presence or absence of H_2O_2 (*middle,* 0.1 mmol/L; *right,* 0.5 mmol/L); EMT was examined by morphologic phenotype or immunoblotting of E-cadherin and ZO-1. *Bar,* 50 μm. *D,* AML-12 cells were treated with TGF-β1 (5 ng/mL) and NAC (10 mmol/L; *top left*) or DFO (100 μmol/L, 24 h; *top right*), and phosphorylated and basal p38 MAPK were detected by immunoblotting. *Bottom left,* mock and FHC siRNA transfected cells were treated with TGF-β1 (5 ng/mL). Phosphorylated and basal p38 MAPK were detected by immunoblotting. *Bottom right*, AML-12 cells were treated with H_2O_2 for 15 min, and phosphorylated and basal p38 MAPK were detected by immunoblotting.

washed with PBS, followed by fixing in 100% methanol at −20°C for 10 min. The samples were subjected to probing with the appropriate primary and secondary antibodies. The nuclei were stained with 4′,6-diamidino-2-phenylindole (DAPI). The fluorescence was visualized under confocal microscopy (Leica).

Migration assays. Cell migration assays were performed using Transwell migration chambers (8 μm pore size; Costar). After treatment, the cells (2×10^4 per Transwell) were plated into the insert in a medium containing 0.5% fetal bovine serum (FBS) and allowed to migrate from upper compartment to lower compartment toward a 10% FBS gradient for 12 h. The cells that remained on top of the filter were scrubbed off, and the cells that migrated to the underside of the filter were fixed in methanol, followed by H&E staining. The migrated cells were counted manually.

Statistical analysis. Quantitative data are expressed as means ± SE. Statistical significance was determined by the two-tailed Student's *t* test or one-way ANOVA, followed by the *LSD-t* test for multiple comparisons. A P value of <0.05 was considered statistically significant.

Materials and some other methods were described in the Supplementary Data.

Results

TGF-β1 down-regulates FHC and leads to an increase in LIP. To screen the proteins involved in EMT, the cellular global proteome profiles of AML-12 cells with or without TGF-β1 treatment were compared using two-dimensional PAGE. More than 2,000 protein spots per gel were displayed after silver nitrate staining (Supplementary Fig. S1*A*). Statistical analysis of three batches of two-dimensional profiles derived from independent experiments showed that 43 spots were significantly

Published OnlineFirst June 16, 2009; DOI: 10.1158/0008-5472.CAN-09-0112

changed (>1.5-fold). A total of 36 spots were successfully identified by MALDI TOF/TOF tandem mass spectrometry (Fig. 1*A*; Supplementary Tables S2 and S3), and they were assigned to six functional categories based primarily on information obtained from Gene Ontology, KEGG (18), and ExPasy (Supplementary Fig. S1*B*).

Among the identified proteins, we found that both FHC and FLC of ferritin were markedly down-regulated by TGF-β1 (Fig. 1*B*). Consistent with the proteomics results, a similar decrease in the amount of FHC protein was detected by immunoblotting, which dropped to an almost undetectable level 48 hours after TGF-β1 treatment in AML-12 (Fig. 1*C*). Moreover, down-regulation of FHC during TGF-β1 treatment was also observed in A549, a human lung adenocarcinoma cell line, and in mouse primary hepatocytes, both of which undergo EMT in response to TGF-β1 (Fig. 1*C*; Supplementary Fig. S2). As the main cellular iron storage protein, the dynamic abundance of ferritin is closely related to LIP levels. It is known that the down-regulation of FHC causes the release of iron from the ferritin complex, which increases the LIP levels (19). As shown in Fig. 1*D*, TGF-β1 induced significant increases in LIP in AML-12 and A549 cells.

The increase in LIP levels is involved in TGF-β1–induced EMT. Desferrioxamine (DFO) is an iron chelator that can effectively impair the cellular LIP level. To investigate whether the increase in LIP caused by iron released from FHC is related to TGF-β1–induced EMT, we first examined the effect of DFO on

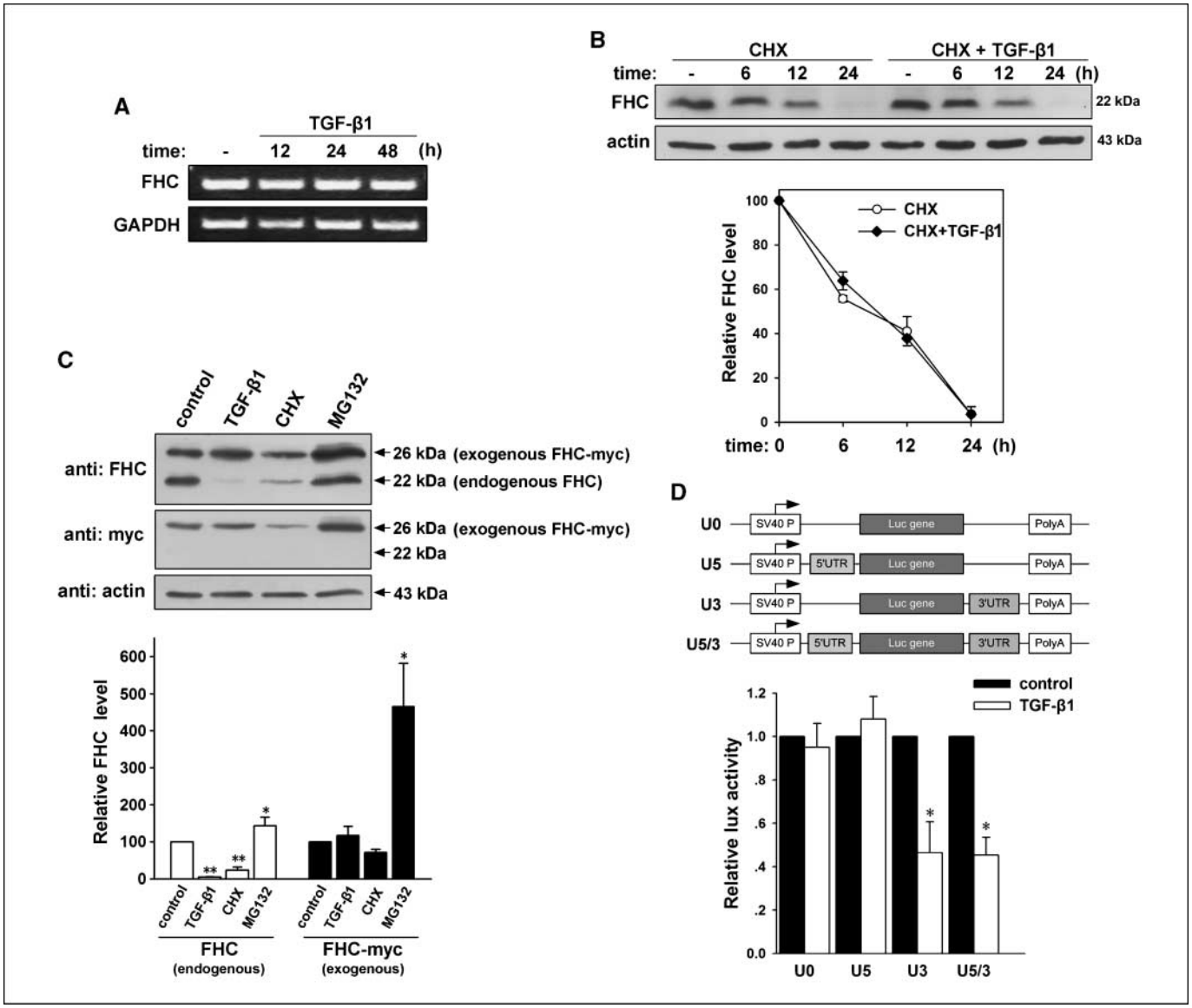

Figure 4. TGF-β1 represses FHC synthesis at the translational level. *A,* FHC and FLC mRNA levels were determined by reverse transcription–PCR in AML-12 cells treated with TGF-β1 (5 ng/mL). GAPDH was used as a control. *B,* AML-12 cells were treated with cycloheximide (*CHX*; 100 μmol/L) in the presence or absence of TGF-β1 (5 ng/mL). FHC levels were examined by immunoblotting (*top*). *Points,* means of the gray intensities of the bands of three independent experiments; *bars,* SE (*bottom*). *C,* AML-12 were transfected with plasmids encoding FHC mRNA without UTR but with a myc-His tag (FHC-myc), then treated with TGF-β1, cycloheximide (*CHX*; 100 μmol/L), or MG132 (10 μmol/L) for 48 h, and analyzed with anti-FHC and anti-myc antibodies (*top*). *Columns,* means of the gray intensities of the bands from three independent experiments; *bars,* SE (*bottom*). **, $P \leq 0.001$; *, $P \leq 0.05$. *D,* the 5′ UTR or/and 3′ UTR of FHC were cloned into the pGL3-control plasmid and transfected into AML-12. The cells were treated with TGF-β1 (10 ng/mL) for 24 h. Luciferase activity assays were carried out. *Columns,* means of the relative fluorescence intensities from three independent experiments; *bars,* SE. *, $P \leq 0.05$.

Published OnlineFirst June 16, 2009; DOI: 10.1158/0008-5472.CAN-09-0112

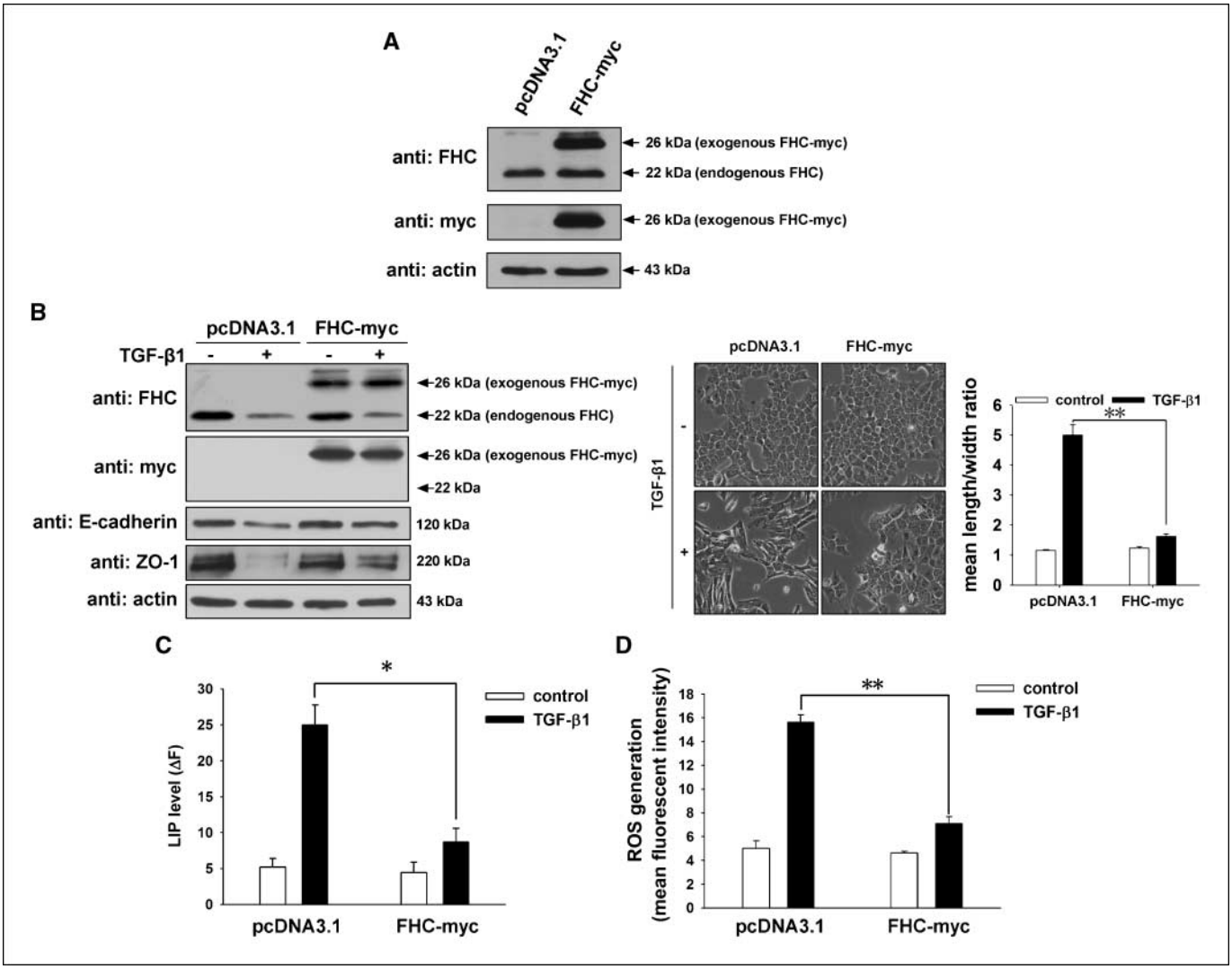

Figure 5. FHC overexpression abolishes TGF-β1–induced LIP increase, ROS production, and EMT. *A,* AML-12 were transfected with a pcDNA3.1 vector and FHC-myc plasmids. FHC levels were determined using anti-FHC or anti-myc antibodies. *B,* immunoblotting of FHC (endogenous and exogenous), E-cadherin, and ZO-1 (*left*); morphologic changes (*middle*); and the average length/width ratio (*right*) in pcDNA3.1 vector and FHC-myc transfected AML-12 after TGF-β1 (5 ng/mL, 48 h) treatment. *C* and *D,* LIP and ROS levels in pcDNA3.1 vector and FHC-myc transfected AML-12 cells after TGF-β1 (5 ng/mL, 24 h) treatment. *, $P \leq 0.05$; **, $P \leq 0.001$.

EMT. In the presence of DFO, TGF-β1–induced up-regulation of fibronectin and down-regulation of E-cadherin were inhibited in both AML-12 and A549 cells (Fig. 2*A*). These results support a role of increased LIP in TGF-β1–induced EMT. To further confirm the role of increased LIP in EMT, we established several RNA interference (RNAi)–stable clones of AML-12 (iFHC; Fig. 2*B*). The knockdown of FHC mitigates the capacity for iron storage of the cells. In iFHC cells, we found that the basal levels of LIP were not elevated (Fig. 2*C*). One possible explanation for this is that the increased LIP resulting from an FHC knockdown might be exhausted during the long periods of iFHC cell clone selection. Because of the very low levels of FHC in iFHC cells, no further FHC down-regulation or iron release can be induced by TGF-β1 in these cells. Thus, compared with vector-transfected cells, iFHC cells lost the ability to increase the LIP in response to TGF-β1 (Fig. 2*C*). Furthermore, we compared the degree of EMT in TGF-β1–treated iFHC cells and control cells. The morphologic changes in the characteristic of EMT were apparently inhibited in iFHC cells 48 hours after TGF-β1 stimulation (Fig. 2*D, top*). The corresponding changes in the levels of EMT marker proteins induced by TGF-β1 were inhibited in iFHC cells (Fig. 2*D, bottom left*). In addition, ZO-1 translocation from the cell membrane to the cytosol and nuclei, another characteristic phenotype of EMT, was also inhibited by FHC knockdown (Fig. 2*D, bottom right*). These results indicate that a TGF-β1–induced elevation of LIP plays an important role in EMT.

LIP participates in EMT via the promotion of ROS production. To further investigate the regulatory mechanism of EMT by LIP elevation, we examined whether TGF-β1–induced EMT is dependent on ROS production catalyzed by elevated LIP. In accordance with the LIP increase, ROS levels markedly increased after TGF-β1 treatment (Fig. 3*A*). The depletion of LIP by DFO apparently inhibits ROS generation (Fig. 3*A*). Next, we examined the effect of NAC, a ROS scavenger, on EMT. NAC inhibited the alterations in the morphology of AML-12 cells in a dose-dependent manner and also abolished TGF-β1–mediated up-regulation of fibronectin and down-regulation of E-cadherin in AML-12 and A549 cells (Fig. 3*B*). Similarly, ROS elevation was not observed in

Published OnlineFirst June 16, 2009; DOI: 10.1158/0008-5472.CAN-09-0112

iFHC cells, in which LIP cannot be elevated in response to TGF-β1 (Fig. 3*C, left*). Interestingly, treatment with H_2O_2, a well-known oxidant that can increase ROS, restored the TGF-β1–induced morphologic changes and down-regulation of E-cadherin and ZO-1 in iFHC cells (Fig. 3*C, middle and right*). Taken together, these results show that LIP participates in TGF-β1–induced EMT through promoting ROS production.

To further confirm the role of LIP and ROS in EMT and investigate the potential downstream mechanism of this pathway in EMT, we examined the activation status of p38 MAPK. TGF-β1 treatment activated p38 MAPK, as shown by its increased phosphorylated form (Fig. 3*D, top left*). SB203580, a p38 MAPK inhibitor, markedly suppressed TGF-β1–induced EMT, and this effect can be generated even 12 or 24 hours after the TGF-β1 induction (Supplementary Fig. S3), indicating that the activation of p38 is critical for EMT. Next, we found that NAC and DFO dramatically inhibited the TGF-β1–induced phosphorylation of p38. Compared with mock-transfected cells, activation of p38 MAPK did not occur in iFHC cells in response to TGF-β1. Moreover, treatment of cells with H_2O_2 alone led to the activation of p38 MAPK (Fig. 3*D*). These results indicated that p38 MAPK is a potential downstream of ROS. TGF-β1 also induces apoptosis in AML-12 cells (20). We found that stable knockdown of FHC or treatment with NAC had no apparent effect on the percentage of apoptosis induced by TGF-β1 (Supplementary Fig. S4), suggesting that FHC-LIP-ROS is not implicated in TGF-β1–induced apoptosis.

TGF-β1 represses FHC synthesis at the translational level. To elucidate the mechanism by which TGF-β1 down-regulates FHC, we investigated the transcription, translation, and degradation of FHC before and after TGF-β1 treatment. As shown in Fig. 4*A*, the FHC mRNA levels remained unchanged and, thus, are apparently not subjected to regulation by TGF-β1. Our data also indicated that there is a constitutive turnover of FHC through lysosome and proteasome pathways. However, TGF-β1 does not down-regulate FHC through promoting FHC degradation (Supplementary Fig. S5).

It has been reported that translational regulation is implicated in the regulation of FHC levels (9, 21, 22). We found that the FHC level was down-regulated by a protein synthesis inhibitor cycloheximide treatment and that treatment of cells with TGF-β1 and cycloheximide together did not enhance the decrease of FHC (Fig. 4*B*), implying that the regulation of FHC by TGF-β1 is at the translational level. To confirm this mechanism, we transfected plasmids encoding myc-tagged FHC (FHC-myc) mRNA without untranslated regions (UTR; the main translational regulation region) into AML-12 cells and found that TGF-β1 cannot down-regulate the exogenous FHC-myc, although there was a significant decrease in endogenous FHC (Fig. 4*C*). Considering that the myc tag may affect the degradable property of exogenous FHC, we treated transfected cells with cycloheximide and MG132, respectively. We found that the exogenous FHC, as well as endogenous FHC, can still be down-regulated by cycloheximide and up-regulated by MG132 (Fig. 4*C*). These results indicate that the inhibitory effect of TGF-β1 on FHC expression depends on the UTRs of FHC mRNA. To test whether it is 5′ UTR or 3′ UTR that is responsible for translational inhibition of FHC by TGF-β1, we attached 5′ UTR or/and 3′ UTR to a luciferase reporter gene and found that the luciferase activity was inhibited by TGF-β1 in cells transfected with plasmids containing 3′ UTR or containing both 3′ UTR and 5′ UTR, but not in cells transfected with only 5′ UTR-containing plasmids (Fig. 4*D*). These results show that TGF-β1 represses FHC synthesis at the translational level and that the 3′ UTR of FHC mRNA is responsible for its translational repression.

Overexpression of FHC abolishes LIP increase, ROS production, and EMT. To further investigate the role of TGF-β1–induced FHC down-regulation in EMT, we examined the effect of overexpression of exogenous FHC, which cannot be down-regulated by TGF-β1 because of a lack of UTRs, on LIP increases, ROS production, and EMT. Figure 5*A* shows the transfection efficiency of exogenous FHC-myc. Compared with transfection of the pcDNA3.1 vector, the overexpression of FHC-myc inhibited the down-regulation of E-cadherin and ZO-1 and EMT-characterized morphologic changes with TGF-β1 treatment (Fig. 5*B*). Moreover, the TGF-β1–induced LIP increase and ROS production were inhibited in FHC-overexpressed AML-12 cells (Fig. 5*C* and *D*). Collectively, these results indicate that TGF-β1–induced FHC down-regulation plays an important role in LIP increase, ROS production, and subsequent EMT.

FHC down-regulation is associated with tumor cell invasiveness and migration. Considering the relationship between EMT and tumor invasion and metastasis, we are interested in whether FHC down-regulation is correlated with tumor invasive and migratory capacities. It has been reported that TGF-β1–mediated EMT plays a role in the invasiveness of esophageal adenocarcinoma (23). We investigated the FHC levels in esophageal cancer tissues using an immunohistochemistry assay. Early-stage carcinoma cells and their adjacent epithelial cells expressed high levels of FHC. However, in advanced-stage carcinoma, especially in scattered and invasive tumor cells, FHC was down-regulated to relatively low levels (Fig. 6*A*). Furthermore, we found that NAC and DFO repressed the TGF-β1–induced migration of A549 human lung adenocarcinoma cell line (Fig. 6*B*). These observations support that FHC down-regulation, and the subsequent regulation of LIP and ROS may contribute to the migratory and invasive capacities of tumor cells.

Discussion

Comparative proteomics approaches can provide a broad view of the molecules involved in various biological processes. We applied proteomics tools to search for new clues elucidating the molecular mechanism of TGF-β1–induced EMT. Among the total 36 significantly altered proteins, some are classic TGF-β1–induced proteins, such as plasminogen activator inhibitor-1 and osteoclast stimulating factor 1, suggesting a high reliability of the data. Furthermore, some of the altered expressed proteins, such as myosin light polypeptide 6 and glucose-6-phosphate-1-dehydrogenase, have also been observed to be differentially expressed during TGF-β–induced EMT in lung cancer cells (24). However, the roles of most of these proteins remain to be characterized.

Ferritin was first identified as the regulator of cellular iron homeostasis. In addition, it has been shown that the regulation of FHC levels and the subsequent changes in LIP and ROS are involved in cell growth arrest, apoptosis, and inflammatory responses (15, 16, 25). In this study, we showed, for the first time, that LIP elevation by TGF-β1–induced repression of FHC plays a key role in EMT. TGF-β1–induced EMT was blocked when LIP elevation was abolished by several methods. First, the treatment of cells with DFO can chelate LIP. Second, in FHC siRNA stably transfected cells, TGF-β1–induced LIP elevation was suppressed through attenuating the cellular iron storage amount. Third, transient overexpression of exogenous FHC also abolished

Published OnlineFirst June 16, 2009; DOI: 10.1158/0008-5472.CAN-09-0112

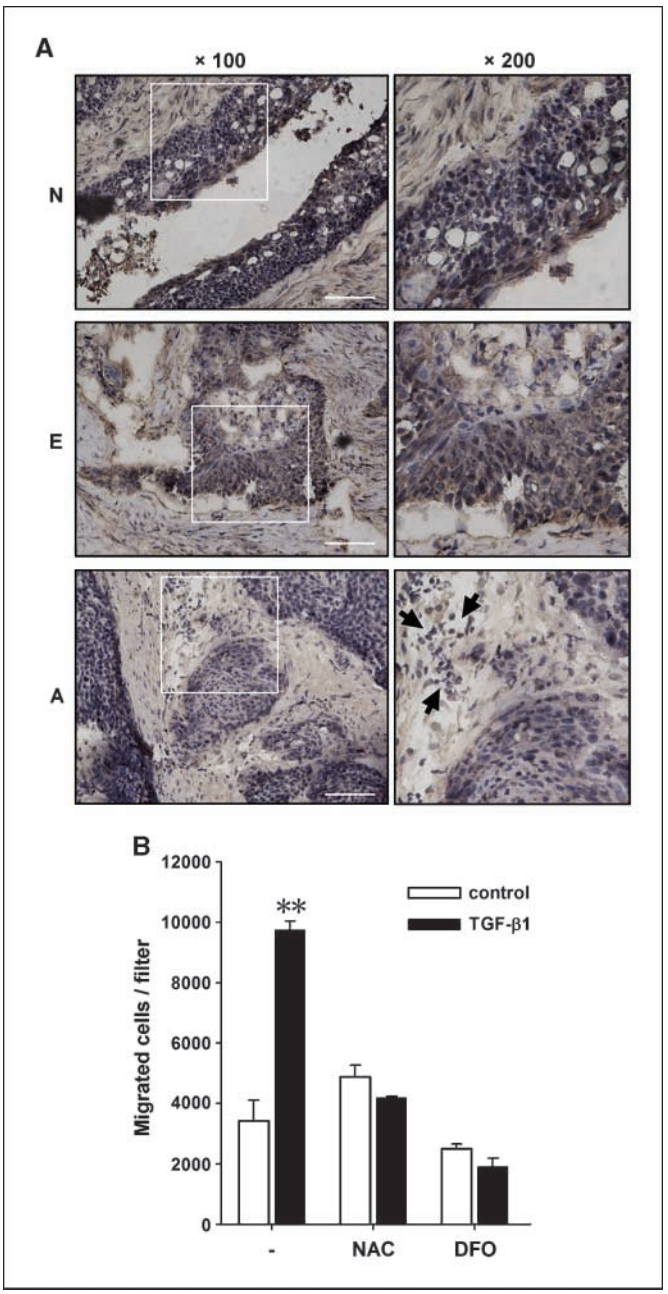

Figure 6. FHC level is associated with tumor cell migration. *A,* representative immunohistochemical staining for the FHC level in normal tissue surrounding carcinoma (*N*), early-stage (*E*), and advanced-stage (*A*) esophageal carcinoma. Nuclei were stained by hematoxylin. *White boxes,* areas selected from the low-power field; *arrows,* scattered and invasive tumor cells. *Scale bar,* 100 μm. *B,* migration of A549 cells in response to TGF-β1 (3 ng/mL, 12 h) with or without NAC (10 mmol/L) or DFO (100 μmol/L). *Columns,* means of migrated cells per filter from three independent experiments; *bars,* SE. **, $P \leq 0.001$.

TGF-β1–induced LIP elevation by sequestering iron. In all of the above cases, TGF-β1–induced EMT was suppressed. Although the LIP elevation is required for TGF-β1–induced EMT, our data also suggest that the increase in LIP level is not sufficient to induce EMT. We observed that transient transfection of FHC RNAi plasmids alone did not induce EMT (data not shown), although knockdown of FHC by RNAi can increase LIP levels (11, 26). This suggests that other TGF-β1–activated signaling events are also critical for EMT.

Ferritin is abundant in some cell lines derived from colon cancer (27), breast cancer (28), and other types of carcinomas (Expression Profile from National Center for Biotechnology Information UniGene database). Nevertheless, it has been reported that FHC level was relatively low in the high metastatic tumor lines compared with the low metastatic lines, which exhibited better differentiated phenotype in bladder tumor model (29) and adenoid cystic carcinoma (30). Consistent with these reports, *in vivo* evidence of esophageal carcinoma showed that FHC levels dropped greatly in advanced-stage tumors, especially in scattered and invasive tumor cells compared with normal tissue and early-stage tumors. These results indicate that the changes in the levels of FHC between early and advanced stages of tumors may be associated with the invasive potential of cancers. Furthermore, because TGF-β1 is abundant in many malignant tumors and TGF-β1–induced EMT plays a role in the invasion of esophageal tumor cells (23), the down-regulation of FHC levels may be induced by TGF-β1 and contribute to EMT induction.

Iron is an essential metal for oxygen transport, electron transport, and for many enzyme-catalyzed reactions. However, *in vitro* and *in vivo* evidence showed that iron can induce carcinogenesis in most cancers and that iron overloading can also be detected in many cancers (31). Efforts have been made to define the manner in which iron levels increase during carcinogenesis. It has been found that tumor cells take up iron at a high rate through increased transferrin receptors and intracellular iron transporters (32). In the present work, we found that TGF-β1 treatment can increase LIP levels in both AML-12 cells and A549 cancer cells, and this effect is dependent on FHC down-regulation. LIP, which accounts for only ~0.2% to 3% of cellular irons, represents a larger hazard than other forms of iron, because it leads directly to cell signaling and response through ROS generation. Because a high level of TGF-β1 is observed in most tumors, increased LIP levels may be related with the high TGF-β1 levels. Additionally, iron chelators have been used as antitumor agents because of their antiproliferation function (33, 34). We also found that DFO significantly inhibited TGF-β1–induced migration of A549 cells, suggesting that high levels of iron in tumors also play a role in tumor progression.

Smad-dependent transcriptional regulations and Smad-independent MAPK activation have been known in TGF-β1–induced EMT (35). ROS has been reported to play an important role in TGF-β1–induced EMT in renal tubular epithelial cells through activation of p38 MAPK (36). In addition, ROS has also been shown to be involved in the mediation of matrix metalloproteinase 3–induced EMT by stimulating the expression of the transcription factor Snail (37). At present, the regulatory mechanism underlying ROS in EMT still remains unclear. In this study, we observed that TGF-β1 induced a ROS increase in normal and cancer cells during EMT and showed that the down-regulation of FHC and the subsequent increase in LIP account for the elevated ROS production. Activation of p38 MAPK has been reported to be an important signaling event induced by TGF-β1 through multiple mechanisms, such as TGF-β1–activated kinase 1 and ROS (38, 39). We confirmed in this study that H_2O_2, as well as TGF-β1, can strongly induce the activation of p38 MAPK. TGF-β1–induced activation of p38 MAPK sustained relative long time period, which is consistent with other reports (39, 40). We also confirmed the role of p38 MPAK in the EMT process, as p38 MAPK inhibitor can potently inhibit EMT even after pretreatment with TGF-β1 for 12 or 24 hours. Furthermore, elimination of LIP and ROS markedly blocked TGF-β1–induced

Published OnlineFirst June 16, 2009; DOI: 10.1158/0008-5472.CAN-09-0112

activation of p38, as well as EMT. These observations suggested that FHC-LIP-ROS pathway is upstream of the p38 MAPK.

During TGF-β1–induced EMT, the dynamic balance of FHC was disrupted by TGF-β1, triggering iron release and subsequent ROS generation. We showed that the disruption of the dynamic balance of FHC by TGF-β1 occurred through the inhibition of FHC translation. Regarding the maintenance of intracellular iron and LIP homeostasis, the known regulatory site of iron responsive elements is located in the 5′ UTR of FHC mRNA (9, 41, 42). Here, we found that TGF-β1 regulates FHC translation via its 3′ UTR, suggesting that different regions of mRNA are responsive to different regulatory signals, through which specific effects can be produced.

In conclusion, we showed that FHC down-regulation and the subsequent LIP increase mediate TGF-β1–induced EMT through ROS generation. The data also indicate that FHC down-regulation is associated with the migratory and invasive phenotypes of tumor cells, suggesting a potential target for the therapeutic control of tumor invasion and progression.

Disclosure of Potential Conflicts of Interest

No potential conflicts of interest were disclosed.

Acknowledgments

Received 1/12/09; revised 4/9/09; accepted 5/6/09; published OnlineFirst 6/16/09.

Grant support: Natural Science Foundation of China grants 30730023, 30721065, and 30623003; National Basic Research Program of China grant 2007CB947900; Shanghai Science Committee grant 06DZ22032; and Creation Foundation from Shanghai Institutes for Life Sciences.

The costs of publication of this article were defrayed in part by the payment of page charges. This article must therefore be hereby marked *advertisement* in accordance with 18 U.S.C. Section 1734 solely to indicate this fact.

We thank Professor Ping Liu for kindly providing deferiprone, Dr. Hong-Bin Ji for assistance in the immunohistochemistry assay, and Dr. Dang-Sheng Li and Guang-Wen Shu for helpful comments and suggestions.

References

1. Thiery JP. Epithelial-mesenchymal transitions in development and pathologies. Curr Opin Cell Biol 2003;15:740–6.
2. Derynck R, Akhurst RJ. Differentiation plasticity regulated by TGF-β family proteins in development and disease. Nat Cell Biol 2007;9:1000–4.
3. Akhurst RJ. TGF β signaling in health and disease. Nat Genet 2004;36:790–2.
4. Zavadil J, Bottinger EP. TGF-β and epithelial-to-mesenchymal transitions. Oncogene 2005;24:5764–74.
5. Batlle E, Sancho E, Franci C, et al. The transcription factor snail is a repressor of E-cadherin gene expression in epithelial tumour cells. Nat Cell Biol 2000;2:84–9.
6. Hajra KM, Chen DY, Fearon ER. The SLUG zinc-finger protein represses E-cadherin in breast cancer. Cancer Res 2002;62:1613–8.
7. Yang J, Mani SA, Donaher JL, et al. Twist, a master regulator of morphogenesis, plays an essential role in tumor metastasis. Cell 2004;117:927–39.
8. Eger A, Aigner K, Sonderegger S, et al. DeltaEF1 is a transcriptional repressor of E-cadherin and regulates epithelial plasticity in breast cancer cells. Oncogene 2005;24:2375–85.
9. Torti FM, Torti SV. Regulation of ferritin genes and protein. Blood 2002;99:3505–16.
10. Kakhlon O, Cabantchik ZI. The labile iron pool: characterization, measurement, and participation in cellular processes(1). Free Radic Biol Med 2002;33:1037–46.
11. Kakhlon O, Gruenbaum Y, Cabantchik ZI. Repression of ferritin expression increases the labile iron pool, oxidative stress, and short-term growth of human erythroleukemia cells. Blood 2001;97:2863–71.
12. Antosiewicz J, Ziolkowski W, Kaczor JJ, Herman-Antosiewicz A. Tumor necrosis factor-α-induced reactive oxygen species formation is mediated by JNK1-dependent ferritin degradation and elevation of labile iron pool. Free Radic Biol Med 2007;43:265–70.
13. Epsztejn S, Glickstein H, Picard V, et al. H-ferritin subunit overexpression in erythroid cells reduces the oxidative stress response and induces multidrug resistance properties. Blood 1999;94:3593–603.
14. Garate MA, Nunez MT. Overexpression of the ferritin iron-responsive element decreases the labile iron pool and abolishes the regulation of iron absorption by intestinal epithelial (Caco-2) cells. J Biol Chem 2000;275:1651–5.
15. Pham CG, Bubici C, Zazzeroni F, et al. Ferritin heavy chain upregulation by NF-κB inhibits TNFα-induced apoptosis by suppressing reactive oxygen species. Cell 2004;119:529–42.
16. Antosiewicz J, Herman-Antosiewicz A, Marynowski SW, Singh SV. c-Jun NH(2)-terminal kinase signaling axis regulates diallyl trisulfide-induced generation of reactive oxygen species and cell cycle arrest in human prostate cancer cells. Cancer Res 2006;66:5379–86.
17. Prus E, Fibach E. Flow cytometry measurement of the labile iron pool in human hematopoietic cells. Cytometry A 2008;73:22–7.
18. Kanehisa M, Goto S. KEGG: Kyoto encyclopedia of genes and genomes. Nucleic Acids Res 2000;28:27–30.
19. Antosiewicz J, Grune T, Kaczor J, Davies KJ. Ubiquitin conjugation is not required for the degradation and elevation of labile iron pool. Free Radic Biol Med 2007;43:311–8.
20. Yang Y, Pan X, Lei W, Wang J, Song J. Transforming growth factor-β1 induces epithelial-to-mesenchymal transition and apoptosis via a cell cycle-dependent mechanism. Oncogene 2006;25:7235–44.
21. Pantopoulos K. Iron metabolism and the IRE/IRP regulatory system: an update. Ann New York Acad Sci 2004;1012:1–13.
22. Rogers JT, Andriotakis JL, Lacroix L, Durmowicz GP, Kasschau KD, Bridges KR. Translational enhancement of H-ferritin mRNA by interleukin-1 β acts through 5′ leader sequences distinct from the iron responsive element. Nucleic Acids Res 1994;22:2678–86.
23. Rees JR, Onwuegbusi BA, Save VE, Alderson D, Fitzgerald RC. *In vivo* and *in vitro* evidence for transforming growth factor-β1-mediated epithelial to mesenchymal transition in esophageal adenocarcinoma. Cancer Res 2006;66:9583–90.
24. Keshamouni VG, Michailidis G, Grasso CS, et al. Differential protein expression profiling by iTRAQ-2DLC-MS/MS of lung cancer cells undergoing epithelial-mesenchymal transition reveals a migratory/invasive phenotype. J Proteome Res 2006;5:1143–54.
25. Xie C, Zhang N, Zhou H, et al. Distinct roles of basal steady-state and induced H-ferritin in tumor necrosis factor-induced death in L929 cells. Mol Cell Biol 2005;25:6673–81.
26. Kakhlon O, Gruenbaum Y, Cabantchik ZI. Repression of the heavy ferritin chain increases the labile iron pool of human K562 cells. Biochem J 2001;356:311–6.
27. Vaughn CB, Weinstein R, Bond B, et al. Ferritin content in human cancerous and noncancerous colonic tissue. Cancer Invest 1987;5:7–10.
28. Higgy NA, Salicioni AM, Russo IH, Zhang PL, Russo J. Differential expression of human ferritin H chain gene in immortal human breast epithelial MCF-10F cells. Mol Carcinog 1997;20:332–9.
29. Vet JA, van Moorselaar RJ, Debruyne FM, Schalken JA. Differential expression of ferritin heavy chain in a rat transitional cell carcinoma progression model. Biochim Biophys Acta 1997;1360:39–44.
30. Zhu N, Yang J, Wang Y, Guan X. Study of the difference of high and low metastasis cell line's gene expression map and metastasis-related genes of adenoid cystic carcinoma. Exp Mol Med 2003;35:243–8.
31. Toyokuni S. Iron-induced carcinogenesis: the role of redox regulation. Free Radic Biol Med 1996;20:553–66.
32. Richardson DR, Ponka P. The molecular mechanisms of the metabolism and transport of iron in normal and neoplastic cells. Biochim Biophys Acta 1997;1331:1–40.
33. Dayani PN, Bishop MC, Black K, Zeltzer PM. Desferoxamine (DFO)-mediated iron chelation: rationale for a novel approach to therapy for brain cancer. J Neurooncol 2004;67:367–77.
34. Le NT, Richardson DR. Iron chelators with high antiproliferative activity up-regulate the expression of a growth inhibitory and metastasis suppressor gene: a link between iron metabolism and proliferation. Blood 2004;104:2967–75.
35. Xu J, Lamouille S, Derynck R. TGF-β-induced epithelial to mesenchymal transition. Cell Res 2009;19:156–72.
36. Rhyu DY, Yang Y, Ha H, et al. Role of reactive oxygen species in TGF-β1-induced mitogen-activated protein kinase activation and epithelial-mesenchymal transition in renal tubular epithelial cells. J Am Soc Nephrol 2005;16:667–75.
37. Radisky DC, Levy DD, Littlepage LE, et al. Rac1b and reactive oxygen species mediate MMP-3-induced EMT and genomic instability. Nature 2005;436:123–7.
38. Zhang YE. Non-Smad pathways in TGF-β signaling. Cell Res 2009;19:128–39.
39. Herrera B, Fernandez M, Roncero C, et al. Activation of p38MAPK by TGF-β in fetal rat hepatocytes requires radical oxygen production, but is dispensable for cell death. FEBS Lett 2001;499:225–9.
40. Yu L, Hebert MC, Zhang YE. TGF-β receptor-activated p38 MAP kinase mediates Smad-independent TGF-β responses. EMBO J 2002;21:3749–59.
41. Eisenstein RS. Iron regulatory proteins and the molecular control of mammalian iron metabolism. Annu Rev Nutr 2000;20:627–62.
42. Rouault TA. The role of iron regulatory proteins in mammalian iron homeostasis and disease. Nat Chem Biol 2006;2:406–14.

Cancer Research
The Journal of Cancer Research (1916–1930) | The American Journal of Cancer (1931–1940)

AACR American Association for Cancer Research

Ferritin Heavy Chain–Mediated Iron Homeostasis and Subsequent Increased Reactive Oxygen Species Production Are Essential for Epithelial-Mesenchymal Transition

Ke-Hua Zhang, Hong-Yu Tian, Xia Gao, et al.

Cancer Res 2009;69:5340-5348. Published OnlineFirst June 16, 2009.